J. Meas. Sci. Instrum., 2025, 16(4): 498-504. http://jmsi.publish.founderss.cn
DOI: 10.62756/jmsi.1674-8042.2025048 jmsi@nuc.edu.cn

Resolving phase errors in microsphere assisted interferometry

HONG Yujian, FU Xiaofeng, SU Zhongyuan, HU Xiaodong*

State Key Laboratory of Precision Measuring Technology and Instruments, Tianjin University, Tianjin 300072, China

***Corresponding author:** HU Xiaodong (xdhu@tju.edu.cn)

Received: November 11, 2024 **Revised:** December 7, 2024 **Accepted:** December 15, 2024

Abstract: Microsphere assisted microscopy (MAM) has been rapidly developed to meet the measurement needs of microstructures. MAM can be integrated with optical interference microscopy (OIM) to achieve high lateral resolution surface profile measurement. However, the microspheres introduce intricate phase changes, resulting in optical path asymmetry which is very challenging to compensate for. This limitation constrains the application of MAM in OIM. In this paper, simulation analysis reveals that the phase transmission of the microsphere is influenced by parameters such as microsphere diameter and its relative position to the sample. It is concluded that a unique compensation process must be adopted for each individual microsphere. Addressing this issue, we proposed a phase compensation algorithm based on the three-dimensional position control of the microsphere and integrated it into our combined system of MAM and white light interferometry (WLI), reducing the phase errors introduced by the microspheres while enhancing the lateral resolution of optical system. This approach improved the profile measurement accuracy, offering a perspective for optically measuring the surface profile of intricate microstructures.

Key words: microsphere assisted microscopy; microsphere assisted interferometry; optical interference microscopy; surface profile measurement; phase compensation

0 Introduction

Optical interference microscopy (OIM) is an extensively used optical measurement method in surface profile measurement[1,2]. It possesses advantages such as planar imaging, non-contact, non-intrusive, and high-precision measurement. However, due to the diffraction limit, the lateral resolution of OIM is significantly lower than its vertical resolution, differing by nearly three orders of magnitude[3,4]. This limitation constrains the practical applications of OIM. Thus, a novel method is demanded to enhance the lateral resolution of the OIM[5,6].

Microsphere-assisted microscopy (MAM) is a promising approach to enhance the lateral resolution of optical systems[7-10]. It is simple to operate, and offers advantages such as easy implementation and compatibility with various optical systems[11,12]. These researches in the field of microsphere imaging consistently demonstrated the remarkable enhancement in resolution capabilities provided by the microsphere[13-16]. Similarly, some researchers have explored the application of MAM in OIM to improve lateral resolution[17-21]. However, their focus has been exclusively on the enhancement of lateral resolution by the microsphere, while overlooking the phase error introduced by the microsphere. This phase error adversely affects the vertical measurement precision of OIM. To address this issue, previous researchers have attempted to compensate for phase errors by using a polynomial 2D fit[22] or placing an identical microsphere in the reference light path[23]. However, due to the differences among the microspheres and the positioning errors of the microspheres, these compensation methods yield limited effectiveness. Furthermore, researchers aspire to operate the microsphere at a distance from the sample surface to enable scanning and enhance the magnification of the microsphere[24-27]. In this operational state, compensating for the phase error of the microsphere becomes even more challenging.

We proposed a microsphere assisted interferometry (MAI) method that combined MAM and OIM. The microsphere was adhered to an atomic force microscope (AFM) cantilever, controlling the three-dimensional position of the microsphere. Simultaneously, we introduced a phase compensation method based on three-dimensional position control to address the challenge of asymmetry introduced by the microsphere in the optical path to eliminate phase errors introduced by the

microsphere. Standard resolution targets and digital video disc (DVD) samples were measured, and the results showed that the algorithm reduced the phase errors introduced by the microsphere and remained effective in lift mode.

1 Theoretical analysis

In order to investigate the phase distribution beneath the microsphere, we used COMSOL multiphysics to analyze the optical field distribution after illumination passes through the microsphere[28]. Considering the production errors of monodisperse microspheres, we selected silica microspheres with diameters of 50 μm and 54 μm as simulation objects. Since the system employed Köhler illumination, the illumination light was set as a plane wave with a wavelength centered at 570 nm, which was the central wavelength of the white-light source. Simulations of intensity and phase of parallel light passing through the microsphere are shown as Fig.1.

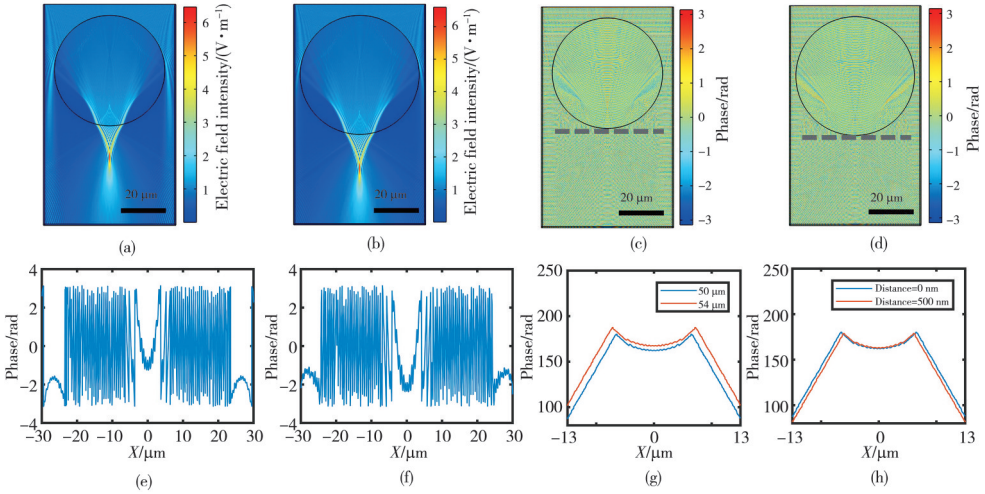

Fig. 1 Simulation of intensity and phase of parallel light passing through microsphere. (a) Electric field intensity by 50 μm silica microsphere; (b) Electric field intensity by 54 μm silica microsphere; (c) Phase distribution by 50 μm silica microsphere (d) Phase distribution by 54 μm silica microsphere; (e) Phase distribution close proximity to surface of 50 μm microsphere (line in (c)); (f) Phase distribution close proximity to surface of 54 μm microsphere (line in (d)). (g) Unwrapped phase of (e) and (f); (h) Unwrapped phase beneath 50 μm microsphere at distances of 0 nm and 500 nm

Fig.1(c) and (d) display the phase distribution with a uniform phase distribution above the microsphere, indicating a significant change in phase after the illumination light passes through the microsphere. In the experiments, the microsphere is placed in close proximity to the sample or at distances of several hundred nanometers. The phase distribution beneath microspheres with different diameters when the distance is 0 nm is shown in Fig.1(e) and (f). To better compare the phase distribution under microspheres with different diameters, we perform phase unwrapping, and the results are presented in Fig.1(g). We observe that the width of the phase distribution is not uniform, and the phase difference varies between different positions. Fig.1(h) shows the phase distribution beneath the 50 μm microsphere when the distance between the microsphere and the sample are 0 nm and 500 nm. The results indicate that there are still differences between the two scenarios.

The simulation results demonstrate that the introduction of the microsphere has a significant impact on the phase, and failure to compensate for it would greatly affect interference measurements. Additionally, the simulation results reveal noticeable differences in the influence of microspheres with different diameters on the phase. For 50 μm and 54 μm microspheres, the phase difference between the center and the edge is 1.9 rad (approximately 172 nm). And there is also a noticeable phase difference when the distance between the microsphere and the sample varies. Furthermore, considering the variations in diameter and sphericity of the microsphere, compensating for the phase impact introduced by microspheres in the interferometric path is challenging based solely on simulated data.

2 Experimental setup

To obtain the profile with enhanced resolution by microsphere and to achieve precise control of the microsphere's three-dimensional position for phase compensation, we establish a system that combines WLI with AFM as shown in Fig.2(a). The interference optical path employs a Linnik-type configuration. Collimating lens L1 transforms the light source into collimated beam. Lens L2 serves as a Köhler illumination lens conjugate with the

objective to ensure uniform sample illumination. Two 10× objectives with numerical aperture (NA) of 0.28 are symmetrically positioned to maintain the symmetry of the interferometric path. The theoretical resolution can be calculated to 1 670 nm ($\delta=0.82\lambda/NA$, where δ denotes resolution, λ is wavelength). The reference mirror M is placed on a piezo actuator PZT2 to generate a 20 nm step. The microsphere is adhered to the side of an AFM cantilever for optical measurement as shown in Fig.2 (b). The sample is placed on the AFM sample stage, and the three-dimensional position of the sample is controlled by a three-dimensional piezo actuator PZT1. The feedback of the AFM can adjust the relative position between the microsphere and the sample when the two in contact, facilitating the selection of the region of interest. When the microsphere comes into contact with the sample, a virtual image magnified by the microsphere is formed beneath the sample surface. After moving the microsphere to the region of interest, it is necessary to readjust the focal plane of the objective to collect the image.

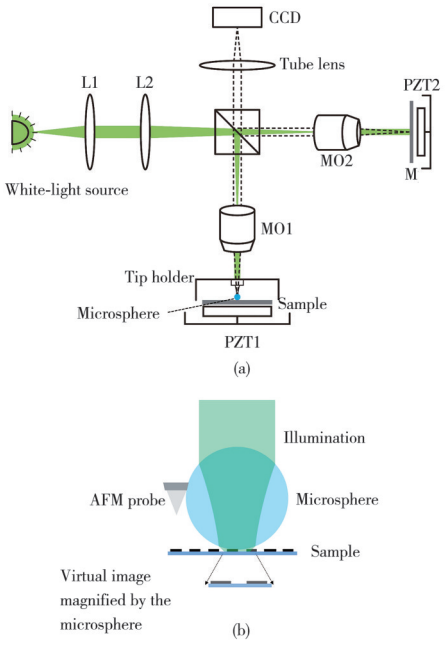

Fig. 2 Combined system. (a) Combined system of MAM and WLI; (b) Microsphere manipulation structure composed of microsphere and AFM cantilever

The resolution enhancement capability of the microsphere slightly decreases with an increase in its diameter, while the field of view expands with the increasing diameter. Microspheres with diameters of 25 μm and 50 μm are experimented with, and the results show no significant difference in resolution. Considering the imaging field of the microsphere and the imaging quality under a 10× objective, the microsphere with a diameter of 50 μm is employed in the experiments described below. The microsphere is adhered to the side of the cantilever with the assistance of AFM, using a cantilever with high K value to withstand the weight of the microsphere.

3 Compensation algorithm

Compensating for the asymmetry introduced by the microsphere poses a challenging problem, primarily due to three main difficulties. Firstly, microspheres themselves exhibit variations in diameter and non-sphericity, even within the same processing batch. It is challenging to find microspheres that are exactly identical, and manufacturing errors between different microspheres can reach 10%. Such discrepancies are unacceptable for interference measurements at the nanometer precision. Consequently, a compensation strategy must be devised for each unique microsphere. Secondly, even for the same microsphere, if its three-dimensional position cannot be precisely controlled, the necessary data for compensation cannot be obtained. Thirdly, due to the complex propagation of light within the microsphere, the influence of the microsphere on the object light wavefront extends beyond mere optical path difference. Therefore, compensating for phase errors introduced by the microsphere cannot be achieved solely by subtracting its height. To address these issues, we employ a differential approach and propose an algorithm based on the three-dimensional position control of the microsphere to eliminate the impact of the microsphere on the symmetry of the interference optical path. During the process of collecting optical signals from the sample, we first adjust the microsphere to its optimal imaging position, capturing white light interference images to obtain the wavefront coupled between the microsphere and the sample

$$O_{MS}(x,y)=O_P(x,y)\times T_M(x,y)\times T_S(x,y), \quad (1)$$

where $O_{MS}(x,y)$ is the object light wavefront calculated by MAI, $O_P(x,y)$ is the plane wave, $T_M(x,y)$ is the wavefront influence function of the microsphere, $T_S(x,y)$ is the wavefront influence function of the sample. At this point, the interference measurement result represents the modulation jointly imposed by the microsphere and the sample. Given that the microsphere has a significant impact on the phase as illustrated in simulation in theoretical analysis, directly using this result as the sample measurement introduces substantial errors. To mitigate this, we adjust the position of the sample stage, moving the microsphere to the standard plane. The standard plane is an optical flat characterized by a uniform surface without height variations or phase changes. The wavefront coupled between the microsphere and the standard plane can be

represented as

$$O_{MP}(x,y)=O_P(x,y)\times T_M(x,y)\times T_P(x,y), \quad (2)$$

where $T_P(x,y)$ is the wavefront influence function of the standard plane. Throughout the movement of the sample stage, the microsphere and the cantilever are stabilized through the feedback system of AFM, ensuring the parameters (x,y) in the formula remain unchanged. The product of the wavefronts after phase conjugation results in

$$O_{MS}(x,y)\times O_{MP}^{*}(x,y)=\left|O_P(x,y)\right|^2\times\left|T_M(x,y)\right|^2\times T_S(x,y)\times T_P^{*}(x,y), \quad (3)$$

where $T_P^{*}(x,y)$ and $T_P(x,y)$ have equal values and they represent a phase-insensitive function. The phase information of the microsphere transfer function is eliminated, allowing for accurate sample signal retrieval through calibration of the phase-insensitive terms.

The precise control of the three-dimensional position of the microsphere is crucial in this compensation algorithm, and it is mainly divided into two parts. Firstly, the position of the microsphere must be precisely controlled to ensure the relative positions of the CCD, objective, and the microsphere remain unchanged. Otherwise, positioning errors of the microsphere will be introduced in phase compensation. Secondly, the relative positions between the microsphere and the sample, as well as between the microsphere and the standard plane, must also remain consistent. Otherwise, changes in the microsphere's own phase transmission, as described in simulation, will be introduced. It is due to the aforementioned two factors that we adopt AFM for precise control of the microsphere's three-dimensional position, thereby enabling the utilization of the complex amplitude multiplication algorithm in MAI.

4 Results and discussion

To validate the effectiveness of the compensation algorithm, standard resolution target Group 9 Element 6 with line widths of 548 nm and period of 1 096 nm is used for imaging, and the measurement results are presented in Fig. 3. First, the white light interference optical path without microspheres needs to be adjusted, focusing on the sample surface and locating the Group 9 of standard resolution targets. At this point, the reference mirror's position is adjusted using a displacement stage to bring the white light interference fringes near the Group 9. Both the object light path and the reference light path have angular adjustment mechanisms to optimize the white light interference fringes.

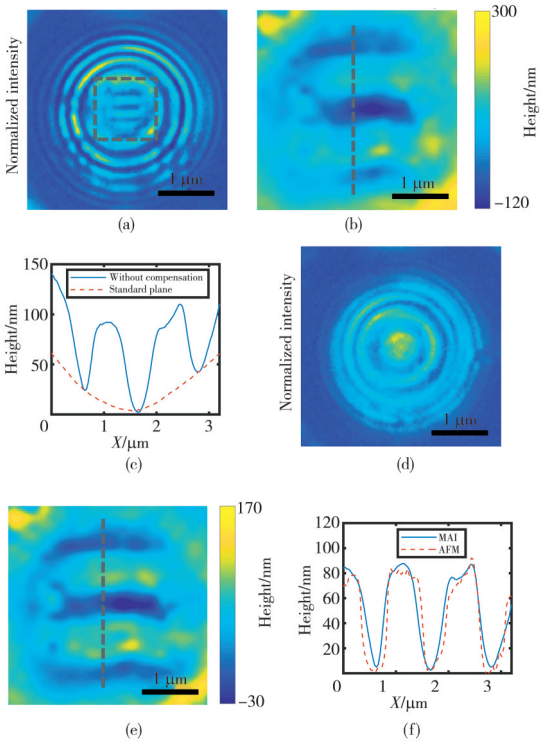

Fig. 3 Profile measurement of resolution target. (a) Interference fringes with microsphere. At this point, microsphere is in close proximity to sample; (b) Height results of resolution target in (a). Results have not been included in the compensation algorithm; (c) Height curve of resolution target (line in b) and standard plane without compensation; (d) Interference fringes of microsphere and standard plane; (e) Height results after applying compensation algorithm; (f) Height curve of line in (e) and AFM results

Next, align the center of the microsphere with the standard resolution target and use the AFM system to engage. Since the optical system's focal plane is on the sample surface before engaging, the virtual image formed by the microsphere lies below the sample surface. After successful probe engaging, adjust the vertical height of the sample stage so that the CCD focuses on the virtual image plane. There is a certain positioning error between the AFM and the optical path system, making it difficult to ensure the microsphere remains in the previously aligned position when it contacts the sample. Additionally, the microsphere's imaging field of view is approximately 9 μm, the field of view might not capture the resolution target information. In this case, the AFM system can be used to scan the sample at low frequency with the microsphere, and gradually adjust the optical path to achieve focus until the target area is focused, as shown in Fig. 3(a). The microsphere disrupts the symmetry of the interference optical path; therefore, it is necessary to readjust the position of the reference mirror to introduce white light interference fringes within the microsphere. Due to the rapid

phase change of the microsphere, the interference fringes are denser. Therefore, the position of the microsphere and the optical path focus should be adjusted before the interference fringes appear, and after introducing the interference fringes, the object light path should no longer be changed.

After implementing the above process, we used the piezo actuator in the reference mirror to control 20 nm steps, completing the WLI measurement. The calculated height measurement results are shown in Fig. 3(b), where the fringes of the resolution target can be clearly distinguished. The microsphere significantly enhances the lateral resolution of WLI, but the vertical information remains inaccurate. Fig. 3(c) shows the height profile of the resolution target, revealing a height difference of nearly 50 nm between the central fringes and the fringes on either side, consistent with the simulation results. To compensate for the phase introduced by the microsphere, after measuring the standard resolution target, the sample stage is adjusted to move the microsphere to a non-structured standard plane. The interference fringes between the microsphere and the standard plane at this position are shown in Fig. 3(d). Since the entire process is conducted under the AFM feedback system, the distance between the microsphere and the sample surface remains unchanged. After applying the phase compensation algorithm, the measurement results of the resolution target by MAI are shown in Fig. 3(e). Fig. 3(f) presents the height information from the line in Fig. 3(e), demonstrating significant improvement over the results without phase error compensation. We also use AFM to measure the resolution target, as indicated in Fig. 3(f), showing good agreement between the optical measurement and the AFM measurement results. From this experiment, it is evident that the introduction of the microsphere enhances the lateral resolution of optical interference. The application of compensation algorithms can significantly reduce height measurement errors introduced by the microsphere.

To demonstrate the effectiveness of the phase compensation algorithm, Fig. 4 shows the phase-error map derived from the uncompensated and the compensated phase maps. As the sample area moves away from the center of the microsphere, the phase error introduced by the microsphere will be larger, and the overall distribution will be symmetrical about the center of the microsphere. From the phase-error map, it can be seen that for MAI, especially when the sample is far away from the center of the microsphere, phase compensation algorithm is necessary.

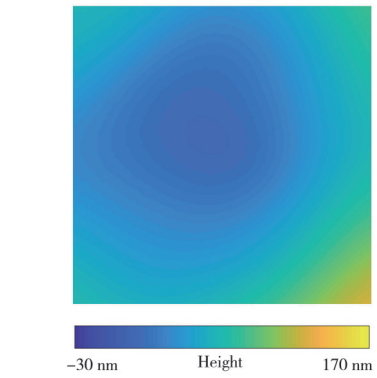

Fig. 4 Phase-error map derived from uncompensated and compensated phase maps

These work demonstrate the measurement results when the microsphere is in contact with the sample. However, in practical measurements, researchers prefer to operate in lift mode, which minimizes the invasiveness of the microsphere on the sample and potentially enhances imaging magnification. To further investigate the measurement capabilities of MAI, we conducted measurements on a DVD when the microsphere was at a distance of 500 nm from the sample, precisely controlled by the feedback of AFM. Since the DVD's period was 735 nm, which was smaller than the resolution target mentioned earlier, we opted for lift mode to measure the DVD to enhance the magnification. Through the experimental steps described above, we obtain height measurement results for the DVD before compensation as shown in Fig. 5.

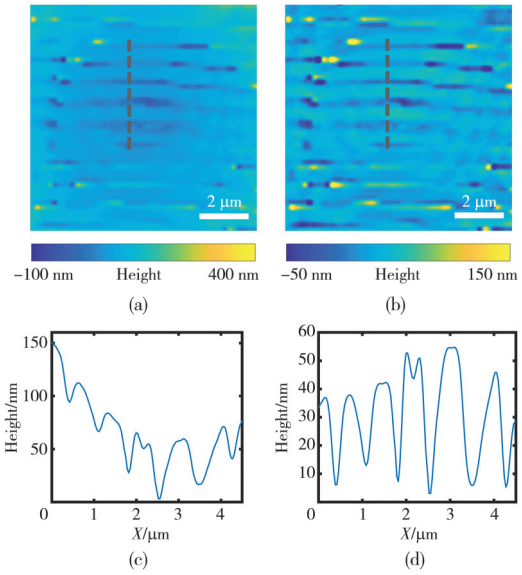

Fig. 5 Profile measurement of DVD. (a) Uncompensated DVD height results; (b) Compensated DVD height results; (c) Height curve of line in (a); (d) Height curve of line in (b)

As the measurement field of view increases, the phase error at the image edges becomes more pronounced. At a

position 2.5 μm away from the center, the phase error has already exceeded 100 nm. However, through the compensation algorithm, we can still eliminate the majority of the error.

In optical microscope, lateral imaging resolution is typically calculated by $\delta=0.61\lambda/NA$, while interference lateral resolution is typically calculated by $\delta=0.82\lambda/NA$. For smaller-sized structures, it is quite possible that image quality might be better than the quality of profile measurements. Hence, there is a situation where DVD is easier to distinguish during imaging, while profile measurements may not be regular as shown in Fig.5(d). Of course, this irregularity could also be related to the quality of the DVD sample itself. However, we can still observe that the compensation algorithm significantly improves the accuracy of height measurements. The results in Fig. 5 demonstrate that the compensation algorithm also works when the microsphere is lifted off the sample, providing a new operating mode for MAI.

The phase compensation process is summarized in Fig.6. The left are the results without phase compensation for the resolution target, while the right are the results for standard plane. With precise control of the microsphere's position by AFM, the microsphere remains stationary in the field of view, and its distance from the sample remains constant, enabling phase compensation.

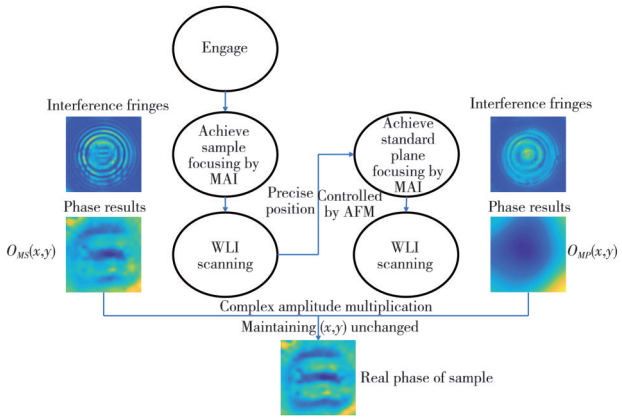

Fig. 6 Phase compensation flowchart

5 Conclusions

We proposed a method that utilized MAM in WLI. To overcome the problem of asymmetric optical paths and inaccurate height measurements introduced by the microsphere, we proposed a phase compensation algorithm based on the three-dimensional position control of the microsphere. This method significantly reduced the impact of the microsphere and enhanced the lateral resolution of the optical system. Through theoretical analysis and experiment, we determined that specific error compensation was essential for each microsphere and this process necessitates precise manipulation of the microsphere's three-dimensional position. We adhered the microsphere to an AFM cantilever, enabling to accurately control its three-dimensional position for error compensation while also allowing for the selection of regions of interest. We used a 50 μm microsphere and a WLI with a theoretical lateral resolution of 1 670 nm, achieving surface profile measurements of a resolution target with period of 1 096 nm and a DVD with period of 735 nm. At the same time, the phase error introduced by the microsphere is compensated, and the phase error can be reduced by 50 nm for the 3 μm×3 μm region. This method opens up possibilities for the application of MAM in OIM, significantly improving the lateral resolution and height measurement accuracy of optical interference systems. It provides a novel approach for optically measuring the surface profile of intricate microstructures.

Acknowledgement

This work was supported by National Natural Science Foundation of China (No. 52275540).

Declaration of conflicting interests

The authors have no conflict of interests related to this publication.

References

[1] YANG S, ZHANG G. A review of interferometry for geometric measurement. Measurement Science and Technology, 2018, 29(10): 102001.

[2] WANG Y, XIE F, MA S, et al. Review of surface profile measurement techniques based on optical interferometry. Optics and Lasers in Engineering, 2017, 93: 164.

[3] TANG M W, LIU X W, WEN Z, et al. Far-field superresolution imaging *via* spatial frequency modulation. Laser & Photonics Reviews, 2020, 14(11): 1900011.

[4] MICÓ V, ZHENG J J, GARCIA J, et al. Resolution enhancement in quantitative phase microscopy. Advances in Optics and Photonics, 2019, 11(1): 135.

[5] KIM M, CHOI Y, FANG-YEN C, et al. Three-dimensional differential interference contrast microscopy using synthetic aperture imaging. Journal of Biomedical Optics, 2012, 17(2): 026003.

[6] PATURZO M, MEROLA F, GRILLI S, et al. Super-resolution in digital holography by a two-dimensional dynamic phase grating. Optics Express, 2008, 16(21): 17107-17118.

[7] CHEN L W, ZHOU Y, LI Y, et al. Microsphere enhanced optical imaging and patterning: From physics to applications. Applied Physics Reviews, 2019, 6(2): 021304.

[8] ZHOU Y, TANG Y, DENG Q Y, et al. Contrast enhancement of microsphere-assisted super-resolution imaging

in dark-field microscopy. Applied Physics Express, 2017, 10(8): 082501.
[9] ZHOU Y, TANG Y, HE Y, et al. Effects of immersion depth on super-resolution properties of index-different microsphere-assisted nanoimaging. Applied Physics Express, 2018, 11(3): 032501.
[10] WU G X, HONG M H. Optical microsphere nano-imaging: progress and challenges. Engineering, 2024, 36: 102-123.
[11] YAN B, WANG Z B, PARKER A L, et al. Superlensing microscope objective lens. Applied Optics, 2017, 56(11): 3142-3147.
[12] YAN B, SONG Y, YANG X B, et al. Unibody microscope objective tipped with a microsphere: design, fabrication, and application in subwavelength imaging. Applied Optics, 2020, 59(8): 2641-2648.
[13] WANG Z B, GUO W, LI L, et al. Optical virtual imaging at 50 nm lateral resolution with a white-light nanoscope. Nature Communications, 2011, 2: 218.
[14] CHEN L W, ZHOU Y, WU M X, et al. Remote-mode microsphere nano-imaging: new boundaries for optical microscopes. Opto-Electronic Advances, 2018, 1(1): 17000101-17000107.
[15] WU G X, ZHOU Y, HONG M H. Sub-50 nm optical imaging in ambient air with 10× objective lens enabled by hyper-hemi-microsphere. Light: Science & Applications, 2023, 12: 49.
[16] KWON S, PARK J, KIM K, et al. Microsphere-assisted, nanospot, non-destructive metrology for semiconductor devices. Light: Science & Applications, 2022, 11: 32.
[17] WANG Y X, GUO S, WANG D Y, et al. Resolution enhancement phase-contrast imaging by microsphere digital holography. Optics Communications, 2016, 366: 81-87.
[18] ABBASIAN V, GANJKHANI Y, AKHLAGHI E A, et al. Super-resolved microsphere-assisted Mirau digital holography by oblique illumination. Journal of Optics, 2018, 20(6): 065301.
[19] LIN Q W, WANG D Y, WANG Y X, et al. Super-resolution quantitative phase-contrast imaging by microsphere-based digital holographic microscopy. Optical Engineering, 2017, 56(3): 034116.
[20] ABBASIAN V, PAHL T, HÜSER L, et al. Microsphere-assisted quantitative phase microscopy: a review. Light: Advanced Manufacturing, 2024, 5(1): 133-152.
[21] DARAFSHEH A, ABBASIAN V. Dielectric microspheres enhance microscopy resolution mainly due to increasing the effective numerical aperture. Light: Science & Applications, 2023, 12: 17-19.
[22] LEONG-HOI A, HAIRAYE C, PERRIN S, et al. High resolution microsphere-assisted interference microscopy for 3D characterization of nanomaterials. Physica Status Solidi (a), 2018, 215(6): 1700858.
[23] PERRIN S, DONIE Y J, MONTGOMERY P, et al. Compensated microsphere-assisted interference microscopy. Physical Review Applied, 2020, 13: 014068.
[24] WANG F F, LIU L Q, YU H B, et al. Scanning superlens microscopy for non-invasive large field-of-view visible light nanoscale imaging. Nature Communications, 2016, 7: 13748.
[25] ZHOU J, LIAN Z X, ZHOU C J, et al. Scanning microsphere array optical microscope for efficient and large area super-resolution imaging. Journal of Optics, 2020, 22(10): 105602.
[26] MASLOV A V, ASTRATOV V N. Resolution and reciprocity in microspherical nanoscopy: point-spread function versus photonic nanojets. Physical Review Applied, 2019, 11(6): 064004.
[27] DUOCASTELLA M, TANTUSSI F, HADDADPOUR A, et al. Combination of scanning probe technology with photonic nanojets. Scientific Reports, 2017, 7: 3474.
[28] YANG H, TROUILLON R, HUSZKA G, et al. Super-resolution imaging of a dielectric microsphere is governed by the waist of its photonic nanojet. Nano Letters, 2016, 16(8): 4862-4870.

微球辅助干涉术中的相位误差补偿方法

洪羽剑, 付晓锋, 苏中元, 胡晓东*

天津大学 精密测试技术及仪器全国重点实验室, 天津 300072

摘　要： 微球辅助显微术得到了迅速发展以实现对微结构的测量。微球辅助显微术可以与光学干涉显微术结合，以实现高横向分辨力的表面形貌测量。然而，微球为干涉光路引入了复杂的相位变化，致使光路不对称，这一误差限制了微球辅助干涉术的应用。本文仿真了微球的相位传输机制，分析了微球直径及其相对于样品的位置对微球相位传输的影响，得出必须对每个微球采用独特的补偿过程这一结论，提出了一种基于微球三维位置调控的相位补偿方法，并将其应用于微球辅助显微和白光干涉测量结合的系统中，减少了微球引入的相位误差，同时提高了光学系统的横向分辨力。该方法提高了微球辅助干涉的表面形貌测量精度，为复杂微结构表面形貌的光学测量提供了新的发展思路。

关键词： 微球辅助显微术；微球辅助干涉术；光学干涉显微术；表面形貌测量；相位补偿

引用格式： HONG Yujian, FU Xiaofeng, SU Zhongyuan, et al. Resolving phase errors in microsphere assisted interferometry. Journal of Measurement Science and Instrumentation, 2025, 16(4): 498-504. DOI: 10.62756/jmsi.1674-8042.2025048